

Spectral study of GX 339-4 with TCAF using Swift/XRT and NuSTAR Observation

Santanu Mondal · Sandip K. Chakrabarti ·
Dipak Debnath

Received: date / Accepted: date

Abstract We fit spectra of galactic transient source GX 339-4 during its 2013 outburst using Two Component Advective Flow (TCAF) solution. For the first time, we are fitting combined NuSTAR and Swift observation with TCAF. We use TCAF to fit 0.8-9.0 keV Swift and 4-79 keV NuSTAR spectra along with the LAOR model. To fit the data we use disk accretion rate, halo accretion rate, size of the Compton cloud and the density jump of advective flows at this cloud boundary as model parameters. From TCAF fitted flow parameters, and energy spectral index we conclude that the source was in the hard state throughout this particular outburst. The present analysis also gives some idea about the broadening of Fe K_α with the accretion rate. Since TCAF does not include Fe line yet, we make use of the ‘LAOR model’ as a phenomenological model and find an estimate of the Kerr parameter to be ~ 0.99 for this candidate.

Keywords X-Rays:binaries · Stars:individual (GX 339-4) · Black Holes · accretion disks · Spectrum · Radiation hydrodynamics

1 Introduction

Transient black hole binaries are ideal objects to study accretion physics. They spend most of the times in the quiescence state and occasionally produce outbursts. Their spectra have mainly two components: a multi-colored black body and a power-law component. The hot Compton cloud [48, 25, 51] close to the black

S. Mondal

Instituto de Física y Astronomía, Facultad de Ciencias, Universidad de Valparaíso, Gran Bretaña N 1111, Playa Ancha, Valparaso, Chile

Indian Centre For Space Physics, 43 Chalanika, Garia Station Road, Kolkata 700084, India

E-mail: santanu.mondal@uv.cl

S. K. Chakrabarti

S.N. Bose National Center for Basic Sciences, JD-Block, Salt Lake, Kolkata, 700098, India Indian Centre For Space Physics, 43 Chalanika, Garia Station Road, Kolkata 700084, India

D. Debnath

Indian Centre For Space Physics, 43 Chalanika, Garia Station Road, Kolkata 700084, India

hole reprocesses soft photons from the disk and produces a power-law tail. Two component advective flow (TCAF) is a self-consistent solution of a viscous transonic flow in presence of radiative transfer. It was shown that [7] flows above a critical viscosity parameter $\alpha = \alpha_{crit}$ will become a Keplerian disk [46], while those below will remain sub-Keplerian. The sub-Keplerian halo creates a high density centrifugal barrier or even passes through a shock close to the black hole. This hot, puffed up region acts as the Compton cloud. Two accretion rates control spectral states of the black hole: if the accretion rate of the disk is large enough to cool down the CENTrifugal pressure supported BOUNDary Layer (CENBOL) which is the post-shock region, one obtains a soft state. The opposite is true for the hard state. The spectral properties of TCAF is studied in [8] and [9]. In certain situations this CENTrifugal pressure dominated BOUNDary Layer or CENBOL exhibits radial and vertical oscillations and thus the Comptonized photon number also oscillates and QPOs are produced. This region is also responsible to produce outflows. A recent review on TCAF could be viewed in [10].

A large number of works attempted to explain evolution of spectral states [50, 44, 39] during outbursts of transient BHCs having temporal and spectral states with phenomenological models, such as disk black-body (DBB), power-law (PL), etc. However, using TCAF, state transitions and the origin of quasi-periodic oscillations (QPOs) have been successfully modelled by our group [16, 40]. In TCAF, oscillations of the post-shock region is either due to the fact that the resonance condition [34, 12] is satisfied, or the Rankine-Hugoniot condition is not satisfied [45]. For transient sources, QPOs evolved monotonically [11, 15, 16] due to the presence of Compton cooling [36] and variation of viscosity [38]. It rises during the rising phase and decreases in the declining phase. After the inclusion of TCAF ([17, 18, 19, 37, 35, 28, 13]) as a local additive Table model in HEASARC's spectral analysis software package XSPEC, physical understanding behind the variation of spectral states in an outburst became easier. TCAF model *fits* is found to be an effective tool to predict dominating (type 'C') QPOs directly from the spectral fitted shock parameters. Mass measurement ([35, 28]) becomes possible from the consideration of constant normalization factor during the fitting of observed data using TCAF. These encouraging aspects motivated us to fit the data with TCAF, even when they may also be fitted with other phenomenological models (e.g., DBB plus PL).

GX 339-4 was first observed in 1973 [30] by 1 – 60 keV MIT X-ray detector onboard OSO-7 satellite. This stellar-mass black-hole binary has a mass function of $M_{bh} \sin(i) = 5.8 \pm 0.5 M_{\odot}$ and low-mass companion of mass $m = 0.52 M_{\odot}$ [27]. We adopt this value throughout the paper. This binary system is located at a distance of $d \geq 6$ kpc [27] with R.A.= $17^h 02^m 49^s.56$ and Dec.= $-48^{\circ} 46' 59''.88$. As the GX 339-4 is a non-eclipsing binary, the inclination angle should be less than 60° [14]. Estimation by [52] gives a lower limit 45° from the secondary mass function. Joint modeling of Suzaku and XMM-Newton observation was used by [33] to explain relativistic broadening of Fe K_{α} line and obtain the spin parameter to be $a = 0.93 \pm 0.01$. Using RXTE and XMM-Newton data, [43] observed a distorted Fe K_{α} line above the continuum. Recently, [42] calculated the value of spin parameter $a = 0.9$ with 33° inclination angle with reflection and disk continuum modeling. Thus the exact values of the disk inclination angle and spin parameter are still doubtful. This required observations through more sensitive and high resolution instruments.

There are extensive discussions on temporal, spectral and multi-wavelength properties of the source during its different outbursts [40,20] using RXTE/PCA observation. Some temporal and spectral properties of this candidate during its 2013 outburst have been discussed by [3] and [23] using NuSTAR and Swift [24] observations with truncated disk model. The authors reported the presence of an Iron line. There are many recent analysis on this object in the literature regarding spectral and timing properties [4]. In this *paper*, for the first time, TCAF model fitting procedure was applied for the combined NuSTAR [26] and Swift observations. Since TCAF represents solutions of governing equations which include radiation mechanism, we expect that fits would yield actual physical parameters such as the accretion rates of two components and the size and other properties of the Compton cloud on the days of the observation. Specifically we want to check whether TCAF also requires an iron line and if so, whether it would be broad double peaked iron line as observed in Suzaku and XMM-Newton observations [32, 5, 49]. Earlier, [1] described very accurately the splitting of red/blue shifted lines from their jet kinematic model (so-called ballistic motion) in SS433. Line profile for Schwarzschild candidates was studied by [22].

The *paper* is organized in the following way: in the next Section, we briefly discuss observation and data analysis procedures using HEASoft and NuSTARDAS software. In §3, we present fitted results obtained from TCAF solution of Swift and NuSTAR data. We also discuss the flow geometry and the nature of the spectral state. From the fitted result, we get some signature of iron line with accretion rate, which also has been discussed. Finally, in §4, we present a brief discussion of our results and make concluding remarks.

2 Observation and Data Analysis

In the present manuscript, we analyze both Swift/XRT and NuSTAR satellite observations of GX 339-4 BHC during its 2013 outburst to obtain TCAF parameters and to check signatures of double peaked Iron line.

2.1 Swift

In our present analysis we use 0.8-9.0 keV Swift/XRT observation of GX 339-4 during 2013 outburst the timings of which match with the NuSTAR observations presented below. The observation IDs are 32490015, 80180001, 80180002, 32898013, and 32988001. We use *xrtpipeline v0.13.2* task to extract the event fits file from raw XRT data. All filtering tasks are done by *FTOOLS*. We analyze XRT Windowed Timing mode data for all the observation. To generate source and background spectra we run *xselect* task. We use *swxwt0to2s6_20130101v015.rmf* file for the response matrix. We rebinned the spectra following the same way as of NuSTAR spectra.

2.2 NuSTAR

We analyze five NuSTAR observations (marked as X02, X04, X06, X08 and X10, where X=800010130 is the initial part of the observation Ids) of BHC GX 339-4.

NuSTAR consists of two independent grazing incidence telescopes which focus X-rays onto corresponding focal planes consisting of Cadmium Zinc Telluride (CZT) pixel detectors. NuSTAR is sensitive to X-ray energies from 4-79 keV and provides high spectral resolution at energies above 10 keV. The two focal planes are referred to as focal plane module (FPM) A and B. NuSTAR data were extracted using the standard NUSTARDAS v1.3.1 software. Each FPM is at the focus of a hard X-ray telescope with a focal length of 10.14 m. We processed the focal plane module A data. We run ‘nupipeline’ task to produce cleaned event lists and ‘nuproducts’ for light curve and spectral file generation. We use 30” radius region for both the source extraction and the background using “ds9”. We group the data using “grppha” command, where we group the whole energy bin with 8 bins in each group. For spectral fitting we use XSPEC [2] version 12.8.1. To fit the spectra with TCAF model in XSPEC, we have a TCAF model generated *fits* file, using theoretical spectra generated by large number of sets of input parameters in modified CT95 code and included it in XSPEC as an additive table model. These parameters are: *i*) mass of the black hole (M_{BH}) in solar mass (M_{\odot}) unit, *ii*) disk rate (\dot{m}_d in Eddington rate, \dot{M}_{Edd}), *iii*) halo rate (\dot{m}_h in \dot{M}_{Edd}), *iv*) size of the Compton cloud (i.e., shock location X_s in Schwarzschild radius r_g), and *v*) density jump in advective flow at Compton cloud boundary (i.e., compression ratio R of the shock). These accretion rates collectively carry information of viscosity inside. Thus we do not need to add viscosity as a separate parameter. This is also a fundamental property of the TCAF model. We use hydrogen column density 5×10^{21} atoms cm^{-2} throughout the analysis as we consider the same mass used in [18], throughout the analysis. All the errors are calculated at 1σ confidence level.

3 Results of model fit

We study Swift/XRT and NuSTAR observations with TCAF solution based fits file which used four physical disk parameters, as we froze the mass at $5.8M_{\odot}$. TCAF solution fitted results are given in Table 1. In Col. 2, we show the MJD of observations, and in Cols. 3, 4, 5 and 6, TCAF fitted parameters such as the disk rate, the halo rate, the shock location and the compression ratio are written. Column 13 gives χ^2 and degrees of freedom. Other Columns are related to the iron lines and discussed below.

3.1 Accretion geometry from TCAF fit

High resolution of Swift and NuSTAR data provides us with a better opportunity to study spectral and line properties using TCAF. In earlier papers, details about TCAF fits have been mentioned and they are not repeated here ([17, 18, 19, 37, 35, 28, 13]). For all observations we use 0.8-9.0 keV Swift/XRT and 4-79 keV NuSTAR data. In Fig. 1(a-d), we present TCAF fitted parameters in the present context. In Fig. 1a, we give variations of the accretion rates of the Keplerian (lower curve; online red circles) and sub-Keplerian (upper curve; online blue circles) components. In these cases the source was in the hard state. In Fig. 1b, we present the variation of the size of the Compton cloud which is the post-shock region of

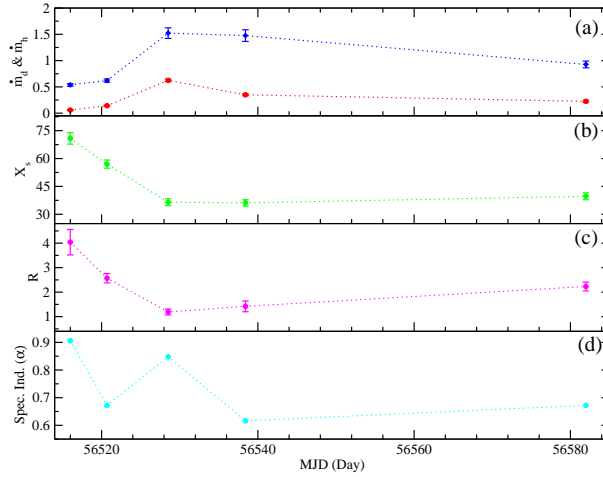


Fig. 1 Variation of (a) TCAF model fitted disk and halo rate, where halo rate is always higher than disk rate, (b) location of the shock (X_s) with day and (c) shock strength, during the 2013 outburst of GX 339-4, using Swift and NuSTAR data. In bottom panel (d) variation of energy spectral index (α) with day.

the sub-Keplerian component [6]. In Fig. 1c, we show the shock strength, i.e., the ratio of the post-shock to pre-shock flow density experienced by the low angular momentum component. This basically carries the information about the density and optical depth inside the Compton cloud. In Fig. 1d, we show the variation of energy spectral index, which clears the hard state of the system throughout. At the beginning of the outburst (MJD=56515.99), the shock was far away from the source and the shock strength was also high (~ 4.04). In the final observation (Id=X10) disk accretion rates were down after ~ 44 days of X08, indicating the end of the outburst. This value is higher than that on X04 day, although relative ratio (halo rate/disk rate) of the accretion rates is higher in the final observed day.

In the first (X02) observed day, the disk rates are less compared to those on other days as the source was in the initial rising phase of the outburst. On X02, when the outburst started, matter was moving with viscous timescale and started to form a Keplerian disk by gradually increasing its rates. The flow was always fully dominated by the sub-Keplerian rate as fresh matters were coming with low angular momentum and since the Compton cloud could not be cooled down, states were always hard. At some point in time, viscosity started going down, and Keplerian disk rate also started declining. As matter supply is reduced, the disk rate became lower also. The whole system was dominated by sub-Keplerian flows throughout.

When it comes to the evolution of the size of the Compton cloud, it is to be remembered that the outer boundary of the Compton cloud is the shock itself. We find that the shock started to move towards the black hole from a location $X_s = 70.83 r_g$ to $\sim 36 r_g$ (where, Schwarzschild radius $r_g = 2GM_{BH}/c^2$) within ~ 24 days on 4th observation (X08 on MJD=56538.41). On the last observation (X10 on MJD=56581.99), the shock again moved away and observed at $\sim 39.68 r_g$ (see, Fig. 1b). The shock compression ratio R ($=\rho_+/\rho_-$, where ρ_+ and ρ_- are post- and pre-shock densities respectively) was always observed to be higher than

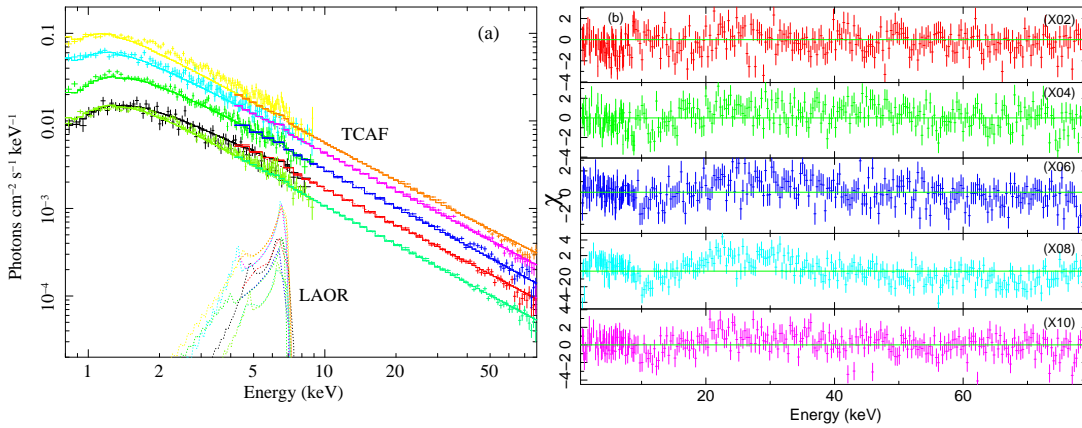


Fig. 2 In (a) unfolded spectra of all the observations fitting with the TCAF model and the LAOR model of double peaked iron line, (b) TCAF and LAOR model fitted residuals for the observations X02-X10 using Swift and NuSTAR data.

unity and became weaker on X06 and X08 observation days. On those days shock was also closer to the black hole. Interestingly, in the whole outburst the shock is within $100 r_g$, in agreement with the results of earlier authors. After that for ~ 44 days there were no observation. It is possible that the source covered other spectral states, such as hard-intermediate, soft-intermediate and soft states but we may have missed them. On the X08 observation day, the shock was found to be receding and becoming strong again. High values of both R and \dot{m}_h indicate that the source was in the hard state during the entire observations. Due to the absence of soft state, we call this as a “failed outburst”. These results are in agreement with [23].

3.2 Spectral analysis using TCAF

For the first time we fit the Swift and NuSTAR observation with TCAF model. As the Swift and NuSTAR have good spectral resolution, data fits well with TCAF solution. In Fig. 2a, unfolded spectra of all the observations after fitting with TCAF and LAOR model [29] of double peaked iron line. From the TCAF model fitted parameters we see that the halo accretion rate is always greater than the disk accretion rate. Thus we infer that the source was in the hard state during this particular outburst. In Fig. 2b, we show the residuals of these fits. Due to the characteristic shape of the double peaked iron line and its very interesting variation with time, we show this separately in Fig. 3. Table 1, gives the fitted parameters from TCAF and LAOR models. The inclination angle was chosen to be $60^\circ - 66^\circ$ (Col. 12) throughout. The emitting region sizes (R_{in} and R_{out}) are also given in the Table. Note that, the inclination angle chosen by us is within the range predicted by other workers discussed in the Introduction. The inner edge of the emitting region gives us the lower limit of the marginally bound orbit. The lowest of $R_{in} = 1.21$ corresponds to the marginally bound orbit of a Kerr black hole of $a = 0.99$ [47].

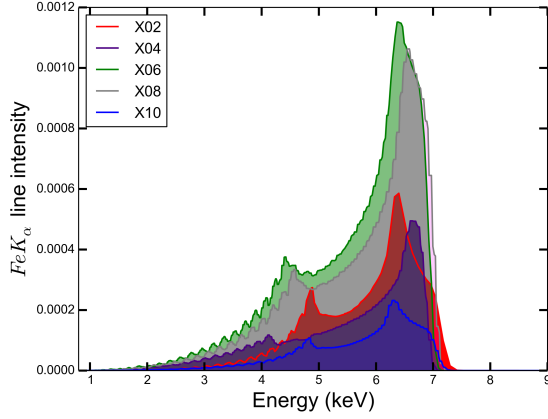


Fig. 3 Variation of $Fe K_{\alpha}$ line intensity of all the observations fitting with the TCAF model and the LAOR model. This variation confirms the signature of double horn line.

4 Concluding Remarks

We have analyzed Swift/XRT and NuSTAR spectra of a very well-known Galactic stellar mass black hole source GX 339-4 during its 2013 outburst using TCAF solution along with LAOR model. We find that as the day progresses, both the accretion rates (\dot{m}_d and \dot{m}_h) increase, the shock moves in (i.e., the Compton cloud slowly collapses due to rapid cooling) and its strength decreases. We observe that the source was in the hard state as the halo rate is always greater than the disk rate and the energy spectral index (α in Col.7) is <1 for all the observed days.

According to [8] and [21], an outburst is triggered due to a sudden rise in viscosity at the outer edge of the disk and is turned off when this viscosity is reduced. If viscosity does not rise above a critical value, the high angular momentum and highly viscous cooler Keplerian disk component does not form [7] and as a result, we may miss the softer states, such as the soft and soft-intermediate spectral states. On the other hand, the most plausible ‘gap’ where these states could have been seen is that between X06 and X08, which appears to be impossible for this object [41, 49, 15, 40]. So, it is likely that the viscosity did not rise above the critical value to have a strong Keplerian component. Furthermore, we find that the residual requires a double peaked iron line produced by a large rotational velocity in all the days, characteristics of the inner region of the flow. The double peak is clearly due to rotation, as the highest intensity of the lines are observed during the highest accretion rate days with relatively smaller size of the Compton cloud. We also observed a significant change in line intensity during the days when the accretion rate is increased and the shock was closer to the black hole (Col. 10 of Table 1). In Col. 9, Laor model fitted power-law emissivity index q is shown. This index indicates different regions of the disk follow different emissivity laws. The present TCAF *fits* file does not include the Iron line and the general relativistic effects. Thus we invoked ‘LAOR model’ as a phenomenological model to understand

Table 1 0.8-9.0 keV and 4-79 keV TCAF+LAOR Model Fitted Parameters

| Id | Day (MJD) | \dot{m}_d | \dot{m}_h | X_s (r_g) | R | α | R_{in} | q | LD | R_{out} | i | χ^2/DOF |
|-----|--------------|-------------------|-------------------|--------------------|-----------------|----------|----------|------|---------|-----------|-------|---------------------|
| (1) | (2) | (3) | (4) | (5) | (6) | (7) | (8) | (9) | (10) | (11) | (12) | (13) |
| X02 | D15.99 | 0.059 ± 0.009 | 0.538 ± 0.025 | 70.83 ± 3.08 | 4.04 ± 0.52 | 0.906 | 5.53 | 2.01 | 8.64E-4 | 61.75 | 64.95 | 766.61/566 |
| X04 | D20.70 | 0.142 ± 0.011 | 0.620 ± 0.030 | 57.01 ± 2.21 | 2.57 ± 0.19 | 0.672 | 1.24 | 2.10 | 6.61E-4 | 16.16 | 62.59 | 917.35/807 |
| X06 | D28.52 | 0.624 ± 0.023 | 1.523 ± 0.101 | 36.52 ± 1.84 | 1.19 ± 0.12 | 0.848 | 1.24 | 1.79 | 1.82E-3 | 30.52 | 64.30 | 784.98/739 |
| X08 | D38.41 | 0.349 ± 0.018 | 1.476 ± 0.111 | 36.13 ± 1.71 | 1.42 ± 0.22 | 0.616 | 1.21 | 1.77 | 1.77E-3 | 46.94 | 61.50 | 1423.99/848 |
| X10 | D81.99 | 0.225 ± 0.020 | 0.927 ± 0.064 | 39.68 ± 1.85 | 2.23 ± 0.18 | 0.672 | 1.24 | 1.73 | 3.17E-4 | 44.85 | 65.00 | 1067.64/875 |

Here X=800010130 and D=565, are the initial part of the observation Ids. and MJDs.

\dot{m}_h , and \dot{m}_d represent TCAF model fitted sub-Keplerian (halo) and Keplerian (disk) rates in Eddington rate respectively. X_s (in Schwarzschild radius r_g), and R are the model fitted shock location and compression ratio values respectively. i , is the disk inclination angle.

LD and q represent Laor model fitted line strength and power-law emissivity index.

the line emission profile and its time variation. According to [29], double-peaked profile is generally produced from the outer part of the disk and the red shifted component dies out at regions very close to the black hole. Based on the present fitted parameters, though not very self-consistently obtained from TCAF solution alone, we find the upper limit of Kerr parameter a of GX 339-4 to be ~ 0.99 and the disk inclination angle is in between $60^\circ - 66^\circ$. In future, we will include these effects and hope to fit the data with TCAF only.

Acknowledgements We are thankful to Dr. Varun Bhalerao for the tutorial of NuSTAR analysis during RETCO-II conference. We are also thankful to the anonymous referee for useful suggestions to improve the quality of the manuscript. SM acknowledges support from a post doctoral grant of the Ministry of Earth Science, Govt. of India and FONDECYT post-doctoral fellowship grand (# 3160350). DD acknowledges support from the project fund of DST sponsored Fast-track Young Scientist (SR/FTP/PS-188/2012). This research has made use of the NuSTAR Data Analysis Software (NuSTARDAS) jointly developed by the ASI Science Data Center (ASDC, Italy) and the California Institute of Technology (Caltech, USA), and the XRT Data Analysis Software (XRTDAS) developed under the responsibility of the ASI Science Data Center (ASDC), Italy.

References

1. Abell, G. O. and Margon, B., A kinematic model for SS433, *Natur*, 279, 701 (1979)
2. Arnaud, K.A., ASP Conf. Ser., Astronomical Data Analysis Software and Systems V, ed. G.H. Jacoby and J. Barnes, 101, 17 (1996)
3. Bachetti, M., et al., No Time for Dead Time: Timing Analysis of Bright Black Hole Binaries with NuSTA, *ApJ*, 800, 109 (2015)
4. Basak, R. and Zdziarski, A. A., Spectral analysis of the XMM-Newton data of GX 339-4 in the low/hard state: disc truncation and reflection, *MNRAS*, 458, 2199 (2016)
5. Brenneman, L. W. & Reynolds, C., Constraining Black Hole Spin via X-Ray Spectroscopy, *ApJ*, 652, 1028 (2006)
6. Chakrabarti, S. K., Standing shocks in isothermal rotating winds and accretion, *MNRAS*, 240, 7 (1989)
7. Chakrabarti, S. K., Standing Rankine-Hugoniot shocks in the hybrid model flows. II - Nonaxisymmetric self-similar solution, *ApJ*, 362, 406(1990)
8. Chakrabarti, S. K. and Titarchuk L.G., Spectral Properties of Accretion Disks around Galactic and Extragalactic Black Holes, *ApJ*, 455, 623 (1995)
9. Chakrabarti, S. K., pectral Properties of Accretion Disks around Black Holes. II. Sub-Keplerian Flows with and without Shocks, *ApJ*, 484, 313 (1997)
10. Chakrabarti, S. K., Turning points in black holes astrophysics, *Astron. Rep.*, 59, 447(2015)

11. Chakrabarti, S. K., Debnath, D. and Nandi, A., et al., Evolution of the quasi-periodic oscillation frequency in GRO J1655-40 - Implications for accretion disk dynamics, *A&A*, 489, L41 (2008)
12. Chakrabarti, S. K., Mondal, S. and Debnath, D., Resonance condition and low-frequency quasi-periodic oscillations of the outbursting source H1743-322, *MNRAS*, 452, 3451(2015)
13. Chatterjee, D., Debnath, D., Chakrabarti, S. K., Mondal, S. and Jana, A., Accretion Flow Properties of MAXI J1543-564 During 2011 Outburst from TCAF Solution, *ApJ*, in press,(2016)
14. Cowley, A. P., Schmidtke, P. C., Hutchings, J. B. and Crampton, D., Optical Observations of the Black Hole Candidate GX 339-4 (V821 Arae), *AJ*, 123, 1741(2002)
15. Debnath, D., Chakrabarti, S. K. and Nandi, A., Properties of the propagating shock wave in the accretion flow around GX339 – 4 in the 2010 outburst, *A&A*, 520, 98(2010)
16. Debnath, D., Chakrabarti, S. K. and Nandi, A., Evolution of the temporal and the spectral properties in 2010 and 2011 outbursts of H 1743-322, *AdSpR*, 52, 2143 (2013)
17. Debnath, D., Chakrabarti, S. K. and Mondal, S., Implementation of two-component advective flow solution in XSPEC, *MNRAS*, 440, L121 (2014)
18. Debnath, D., Mondal, S. and Chakrabarti, S.K., Characterization of GX 339-4 outburst of 2010-11: analysis by XSPEC using two component advective flow model, *MNRAS*, 447, 1984(2015a)
19. Debnath, D., Molla, A.A., Chakrabarti, S.K. and Mondal, S., Accretion Flow Dynamics of MAXI J1659-152 from the Spectral Evolution Study of its 2010 Outburst using the TCAF Solution, *ApJ*, 803, 59 (2015b)
20. Dincer, T., Kalemci, E. and Buxton, M. M., et al., X-Ray, Optical, and Infrared Observations of GX 339-4 during Its 2011 Decay, *ApJ*, 753, 55(2012)
21. Ebisawa, K., Titarchuk, L.G. and Chakrabarti, S.K., On the Spectral Slopes of Hard X-Ray Emission from Black Hole Candidates, *PASJ*, 48, 59(1996)
22. Fabian, A. C., Rees, M. J., Stella, L. and White, N. E., X-ray fluorescence from the inner disc in Cygnus X-1, *MNRAS*, 238, 729(1989)
23. Fürst, F., Nowak, M. A., Tomsick, J., Miller, J.M., et al., The Complex Accretion Geometry of GX 339-4 as Seen by NuSTAR and Swift, *ApJ*, 808, 122(2015)
24. Gehrels et al., The Swift Gamma-Ray Burst Mission, *ApJ*, 611, 1005(2004)
25. Haardt, F. and Maraschi, L., X-ray spectra from two-phase accretion disks, *ApJ*, 413, 507(1993)
26. Harrison, F. A., Craig W. W., Christensen F.E., Hailey C.J., Zhang, W. W., et al., The Nuclear Spectroscopic Telescope Array (NuSTAR) High-energy X-Ray Mission, *ApJ*, 770, 103 (2013)
27. Hynes, R. I., Steeghs, D. and Casares, J., et al., Dynamical Evidence for a Black Hole in GX 339-4, *ApJ*, 583, L95(2003)
28. Jana, A., Debnath, D., Chakrabarti, Mondal, S., Molla, A., Accretion Flow Dynamics of MAXI J1836-194 During Its 2011 Outburst from TCAF Solution, *ApJ*, 890, 107(2016)
29. Laor, A., Line profiles from a disk around a rotating black hole, *ApJ*, 376, 90(1991)
30. Markert, T. H., Canizares, C. R. and Clark, G. W. et al., Observations of the Highly Variable X-Ray Source GX 339-4, *ApJ*, 184, L67(1973)
31. McClintock, J. E. and Remillard, R. A., in *Compact Stellar X-ray Sources*, Cambridge, Astrophysical Ser., vol. 39, ed. W. Lewin & M. van der Klis, Cambridge Univ. Press, 157(2006)
32. Miller, J. M., Homan, J., Steeghs, D., Rupen, M. et al., A Long, Hard Look at the Low/Hard State in Accreting Black Holes, *ApJ*, 653, 525(2006)
33. Miller, J., et al., Initial Measurements of Black Hole Spin in GX 339-4 from Suzaku Spectroscopy, *ApJ*, 679, L113(2008)
34. Molteni, D., Sponholz, H. and Chakrabarti, S. K., Resonance Oscillation of Radiative Shock Waves in Accretion Disks around Compact Objects, *ApJ*, 457, 805(1996)
35. Molla, A., Debnath, D., Chakrabarti, Mondal, S., Estimation of Mass of the Black Hole Candidate MAXI J1659-152 using TCAF and POS Models, *MNRAS*, 460, 3163(2016)
36. Mondal, S., and Chakrabarti, S. K., Spectral properties of two-component advective flows with standing shocks in the presence of Comptonization, *MNRAS*, 431, 2716(2013)
37. Mondal, M., Debnath, D. and Chakrabarti, S. K., Inference on Accretion Flow Dynamics Using TCAF Solution from the Analysis of Spectral Evolution of H 1743-322 during the 2010 Outburst, *ApJ*, 786, 4(2014)
38. Mondal, M., Chakrabarti, S. K. and Debnath, D., Is Compton Cooling Sufficient to Explain Evolution of Observed Quasi-periodic Oscillations in Outburst Sources?, *ApJ*, 798, 57(2015)

39. Motta, S., Belloni, T. and Homan, J., The evolution of the high-energy cut-off in the X-ray spectrum of GX 339-4 across a hard-to-soft transition, *MNRAS*, 400, 1603(2009)
40. Nandi, A., Debnath, D., Mandal, S., et al., Accretion flow dynamics during the evolution of timing and spectral properties of GX 339-4 during its 2010-11 outburst, *A&A*, 542, 56 (2012)
41. Nowak, M. A., Wilms, J. and Dove, J. B., Low-Luminosity States of the Black Hole Candidate GX 339-4. II. Timing Analysis , *ApJ*, 517, 355(1999)
42. Plant, D. S., Fender, R. P., Ponti, G., Muñoz-Darias, T. and Coriat, M., Revealing accretion on to black holes: X-ray reflection throughout three outbursts of GX 339-4, *MNRAS*, 442, 1767(2014)
43. Reis, R. C., et al., A systematic look at the very high and low/hard state of GX339-4: constraining the black hole spin with a new reflection model, *MNRAS*, 387, 1489(2008)
44. Remillard, R. A. and McClintock, J. E., X-Ray Properties of Black-Hole Binaries, *ARA&A*, 44, 49(2006)
45. Ryu, D., Chakrabarti, S. K. and Molteni, D., Zero-Energy Rotating Accretion Flows near a Black Hole, *ApJ*, 474, 378(1997)
46. Shakura, N. I. and Sunyaev, R. A., Black holes in binary systems. Observational appearance, *A&A*, 24, 337 (1973)
47. Shapiro, S. and Teukolosky, S., *Black Holes, Neutron Stars and White Dwarfs*, 361, John Wiley & Sons, New York (1983)
48. Sunyaev, R. A. and Titarchuk, L. G., Comptonization of X-rays in plasma clouds - Typical radiation spectra, *ApJ*, 86, 121 (1980)
49. Tomsick et al., Broadband X-Ray Spectra of GX 339-4 and the Geometry of Accreting Black Holes in the Hard State, *ApJ*, 680, 593(2008)
50. van der Klis, M., The QPO phenomenon, *AN*, 326, 798(2005)
51. Zdziarski, A. A., Lubinski, P., Gilfanov, M. and Revnitsev, M., Correlations between X-ray and radio spectral properties of accreting black holes, *MNRAS*, 342, 355(2003)
52. Zdziarski, A. A., Gierliński, M., Mikolajewska, J., Wardziński, G., Smith, D. M., Harmon, B. A. and Kitamoto, S., X 339-4: the distance, state transitions, hysteresis and spectral correlations, *MNRAS*, 351, 791(2004)